

# Electrical characteristics of $^{60}\text{Co}$ $\gamma$ -ray irradiated MIS Schottky diodes

A. Tataroğlu \*, Ş. Altındal

*Department of Physics, Faculty of Arts and Sciences, Gazi University, 06500 Ankara, Turkey*

Received 19 May 2006; received in revised form 8 August 2006

Available online 18 September 2006

## Abstract

In order to interpret the effect of  $^{60}\text{Co}$   $\gamma$ -ray irradiation dose on the electrical characteristics of MIS Schottky diodes, they were stressed with a zero bias at 1 MHz in dark and room temperature during  $\gamma$ -ray irradiation and the total dose range was 0–450 kGy. The effect of  $\gamma$ -ray exposure on the electrical characteristics of MIS Schottky diodes has been investigated using  $C$ – $V$  and  $G/\omega$ – $V$  measurements at room temperature. Experimental results show that  $\gamma$ -ray irradiation induces a decrease in the barrier height  $\Phi_B$  and series resistance  $R_s$ , decreasing with increasing dose rate. Also, the acceptor concentration  $N_A$  increases with increasing radiation dose. The  $C$ – $V$  characteristics prove that there is a reaction for extra recombination centers in case of MIS Schottky diodes exposed to  $\gamma$ -ray radiation. Furthermore, the density of interface states  $N_{ss}$  by Hill–Coleman method increases with increasing radiation dose. Experimental results indicate that the interface-trap formation at high irradiation dose is reduced due to positive charge build-up in the Si/SiO<sub>2</sub> interface (due to the trapping of holes) that reduces the flow rate of subsequent holes and protons from the bulk of the insulator to the Si/SiO<sub>2</sub> interface.

© 2006 Elsevier B.V. All rights reserved.

*PACS:* 61.80.Ed; 07.85.–m; 73.40.Qv; 84.37.+q; 61.80.–x; 73.20.–r

*Keywords:*  $\gamma$ -Ray effects; MIS Schottky diodes;  $C$ – $V$  and  $G/\omega$ – $V$  characteristics; Interface states; Series resistance

## 1. Introduction

Metal–insulator–semiconductor (MIS)-type Schottky diodes and metal–oxide–semiconductor (MOS) capacitors consist of a semiconductor substrate covered by an oxide layer upon which a metal electrode gate is deposited. The presence of this interfacial insulator layer between metal and semiconductor makes them rather sensitive to irradiation (such as  $^{60}\text{Co}$   $\gamma$ -ray, high-level electrons, neutrons or ions). Most of the radiation-induced damages are located at or near the Si/SiO<sub>2</sub>. Since the high-energy particles irradiated enter these devices or exposure dose greater than a kilorad, the considerable amount of lattice defects such as vacancies, interstitials; complex defects are induced in

semiconductor materials. These defects act as a recombination centers trapping the generated carriers. These defects that act as recombination centers or minority/majority carrier trapping centers cause degradation of the diode performance and applications. Recently, several groups have investigated the effect of radiation on this kind of devices [1–16].

These devices are required to have radiation-resistant characteristics. Therefore, it is of interest to investigate the damage defect centers on the performance of these types of semiconductor devices. Further, improvements in radiation resistance of MIS and MOS structures are necessary for widespread  $\gamma$ -ray irradiation dose on their electrical characteristics [1–16]. The origins of the radiation-induced defects are not clearly understood and further studies are necessary to clarify the atomic structure of the defects. However, fundamental studies on radiation-induced defects in Si have extensively been carried out by

\* Corresponding author. Tel.: +90 312 212 6030; fax: +90 312 212 279.  
E-mail address: [ademt@gazi.edu.tr](mailto:ademt@gazi.edu.tr) (A. Tataroğlu).

Bourgoin and Corbett [17] and Kimerling [18]. Nicollian and Goetzberger [16] argued that charge trapped within 30 Å of the interface could produce fluctuations in surface potential capable of trapping electrons and holes.

The density of interface states between metal and semiconductor interfaces in the MIS-type Schottky diodes has been studied more than that in the MS Schottky diodes due to the existence of interfacial insulator layer between metal and semiconductor that passivates the surface of semiconductor in MIS-type Schottky diodes. Winokur et al. [12–14], Zaininger and Holmes-Siedle [4] and Ma [1,10] were among the first to make a systematic observation of the after-irradiation behavior of radiation-induced interface traps in MIS and MOS devices. Interface traps, also referred to as interface states or surface states, are electronic energy levels located at the MIS interface and they are important parameters like series resistance. Especially, there are two important effects of radiation: the transient effects are due to the electron–hole pair generation and permanent effect is due to the bombardment of devices with radiation which causes changes in the crystal lattice. The radiation-generated holes may diffuse in the insulator, but are less mobile than the electrons; many stationary hole traps are also present.

In this work, in order to clarify the  $^{60}\text{Co}$   $\gamma$ -ray irradiation effects on the electrical characteristics of the Al/SiO<sub>2</sub>/p-Si Schottky diodes, we exposed a maximum cumulative dose of 450 kGy on diode at room temperature. After each dose rate, we report on the changes in electrical characteristics evaluated using forward and reverse bias capacitance–voltage ( $C$ – $V$ ) and conductance–voltage ( $G/\omega$ – $V$ ) measurements. The degradation observed in the reverse bias  $C$ – $V$  and  $G/\omega$ – $V$  characteristics is due to an increasing in radiation-induced defects. In addition, experimental results for the Al/SiO<sub>2</sub>/p-Si (MIS) Schottky diode are compared with results published for these types of semiconductor devices.

## 2. Experimental detail

The Al/SiO<sub>2</sub>/p-Si (MIS) Schottky diodes used in this study were fabricated using boron-doped single crystals silicon wafer with (100) surface orientation having thickness of 280  $\mu\text{m}$ , 2 in. diameter and 8  $\Omega\text{cm}$  resistivity. For the fabrication a process, Si wafer was degreased in organic solvent of  $\text{CHCl}_3$ ,  $\text{CH}_3\text{COCH}_3$  and  $\text{CH}_3\text{OH}$  consecutively and then etched in a sequence of  $\text{H}_2\text{SO}_4$  an  $\text{H}_2\text{O}_2$ , 20% HF, a solution of  $6\text{HNO}_3$ :1HF:35 $\text{H}_2\text{O}$ , 20% HF and finally quenched in de-ionized water for a prolonged time. Preceding each cleaning step, the wafer was rinsed thoroughly in de-ionized water of resistivity of 18 M $\Omega\text{cm}$ .

Immediately after surface cleaning, to form ohmic contacts on the back surface of the Si wafer, high purity Al metal (99.999%) with a thickness of  $\sim 2000$  Å was thermally evaporated from the tungsten filament onto the whole back surface of the Si wafer in the pressure of  $\sim 2 \times 10^{-6}$  Torr in oil vacuum pump system and the evaporated aluminium (Al) was sintered. The oxidations are

carried out in a resistance-heated furnace in dry oxygen with a flow rate of a 2 l/min and the oxide layer thickness is grown at the temperatures of 700 °C within 60 min. To form the Schottky contacts, the circular dots of  $\sim 1$  mm diameter and  $\sim 2000$  Å thick Al are deposited onto the oxidized surface of the wafer for through a metal shadow mask in a liquid nitrogen trapped vacuum system in a vacuum of  $\sim 2 \times 10^{-6}$  Torr. The interfacial insulator layer thickness was estimated to be about 34 Å from high frequency (1 MHz) measurement of the interface insulator capacitance in the strong accumulation region for MIS Schottky diode [15].

The capacitance–voltage ( $C$ – $V$ ) and conductance–voltage ( $G/\omega$ – $V$ ) measurements were carried out using an HP 4192A LF impedance analyzer (5 Hz–13 MHz). The ac signal was generated by a low-distortion oscillator with the amplitude attenuated to 50 mV<sub>rms</sub> to meet the small signal requirement for thin oxide capacitors. The  $C$ – $V$  and  $G/\omega$ – $V$  measurements were performed before and after  $^{60}\text{Co}$   $\gamma$ -ray source irradiation with the dose of 2.12 kGy/h and total dose range was 0–450 kGy at room temperature and 1 MHz. All measurements were carried out with the help of a microcomputer through an IEEE-488 ac/dc converter card.

## 3. Results and discussion

Analysis of the capacitance–voltage ( $C$ – $V$ ) characteristics was realized using the expression for the bias dependence of the depletion capacitance,  $C$ , of the MIS Schottky diodes. In MIS Schottky diodes the depletion layer capacitance is given as follows [19–21]:

$$C^{-2} = \frac{2(V_d + V)}{\epsilon_s \epsilon_0 q A^2 N_A}, \quad (1)$$

where  $A$  is the area of rectifier contact,  $\epsilon_s$  is the permittivity of semiconductor (Si),  $\epsilon_0$  is the permittivity of the free space,  $N_A$  is the carrier (acceptor) concentration,  $q$  is the electronic charge,  $V_d$  is the diffusion potential at zero bias and  $V$  is the magnitude of the applied bias. The values of  $V_0$  and  $N_A$  can be obtained from the intercept and slope of  $C^{-2}$  versus  $V$  plot by means of Eq. (1).

The value of the barrier height ( $\Phi_B$ ) can be obtained by the relation,

$$\Phi_B = V_0 + kT/q + E_F - \Delta\Phi_B, \quad (2)$$

where  $E_F$  is the energy difference between the bulk Fermi level and valance band edge and  $\Delta\Phi_B$  is the image force barrier lowering and can be obtained from the well-known relationship in [19,20,22].

Fig. 1 shows a typical  $C$ – $V$  relation obtained from the measurement at a high frequency of 1 MHz in dark and room temperature before and after  $\gamma$ -ray irradiation, which manifests the presence of the trapping centers [21,23,24]. It is clear that for p-type substrate, holes accumulate underneath SiO<sub>2</sub> at negative gate bias. The shift of the  $C$ – $V$  data

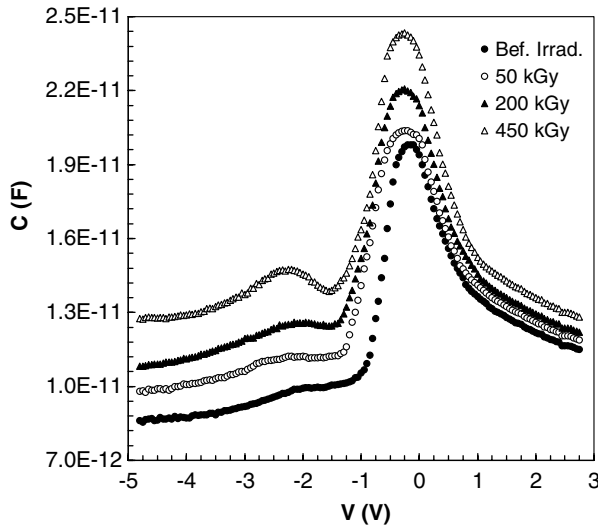


Fig. 1. The  $C$ – $V$  characteristics of the Al/SiO<sub>2</sub>/p-Si (MIS) Schottky diodes before and after  $\gamma$ -ray irradiation obtained at 1 MHz and room temperature.

from inversion toward the accumulation region increases with the increase in radiation dose. By analyzing the high frequency curves in Fig. 1, two apparent effects can be distinguished: (a) shifting of the maximum of the capacitance value to the negative voltage and stretch-out of the  $C$ – $V$  curves, reflecting the generation of oxide charge due to electron–hole pair generation by the radiation and (b) the increasing values of the capacitance with increasing dose of ionizing radiation [6,25].

The  $C$ – $V$  curves also give a peak in the depletion region due to the effect of series resistance and particular distribution of interface states between Si/SiO<sub>2</sub> interface. Therefore, depending on the relaxation time of the density of interface states ( $N_{ss}$ ) and the frequency of the ac signal, there may be a capacitance due to interface states in excess to depletion layer capacitance. As a result we can say that in the low frequencies  $N_{ss}$  can follow the ac signal and yield an excess capacitance, which depends on the frequency, but in the high frequency limit ( $f \geq 500$  kHz), the interface states cannot follow the ac signal. This makes the contribution of interface state capacitance to the total capacitance negligibly small [26,27]. Therefore, the  $C$ – $V$  measurements are carried out at sufficiently high frequency of 1 MHz.

Fig. 2 shows the reciprocal of the squared capacitance per unit area as a function of the bias before and after  $\gamma$ -ray irradiation between 0 and 450 kGy. As can be seen in Fig. 2,  $C^{-2}$ – $V$  variation is linear in the wide voltage range of 0–0.75 V at sufficiently high frequency (such that carrier life time  $\tau$  is much larger than  $1/2\pi f$ ) [20]. This linearity of the curve is attributed to the uniformity of the  $N_A$  in the depletion region, since the interface states cannot follow ac signal at high frequencies.

The calculated values of  $V_0$ ,  $V_d$ ,  $N_A$ ,  $E_F$ ,  $\Delta\Phi_B$  and  $\Phi_B$ , obtained from  $C^{-2}$ – $V$  plot at different irradiation dose ranges, are presented in Table 1.

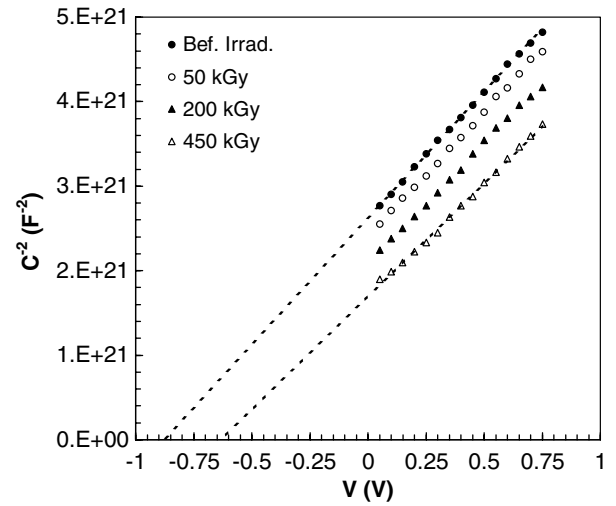


Fig. 2.  $C^{-2}$ – $V$  characteristics plot for the Al/SiO<sub>2</sub>/p-Si (MIS) Schottky diodes at 1 MHz before and after  $\gamma$ -ray radiation.

As shown in Table 1, before and after exposure of 450 kGy dose, the  $C$ – $V$  measurements revealed that the values of barrier height ( $\Phi_B$ ) changes between 1.193 and 0.937 eV and the carrier concentration  $1.59 \times 10^{14}$  to  $1.75 \times 10^{14} \text{ cm}^{-3}$ . The  $\Phi_B$  values including the effect of  $\gamma$ -ray exposure on the  $C$ – $V$  is shown in Fig. 3, where it is clear that the intercept of the  $C^{-2}$  versus  $V$  characteristics

Table 1

Electrical parameters of MIS Schottky diodes obtained before and after irradiation between 0 and 450 kGy

Irradiation (kGy)	$V_0$ (V)	$V_d$ (eV)	$N_A$ ( $\times 10^{14} \text{ cm}^{-3}$ )	$E_F$ (eV)	$\Delta\Phi_B$ (meV)	$\Phi_B$ (eV)
Before irradiation	0.882	0.908	1.59	0.294	9.005	1.193
50	0.811	0.837	1.60	0.294	8.834	1.122
200	0.732	0.758	1.67	0.293	8.710	1.043
450	0.628	0.654	1.75	0.292	8.509	0.937

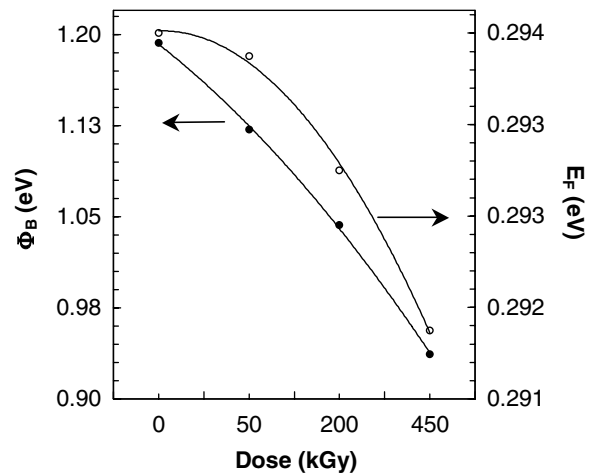


Fig. 3. Barrier height ( $\Phi_B$ ) and  $E_F$  plots obtained from the reverse bias  $C^{-2}$ – $V$  versus as a function of cumulative  $\gamma$ -ray doses.

changes with increasing total dose, shifting to more positive voltages. The decrease in barrier height,  $\Phi_B$ , obtained from the experimental  $C^{-2}$ - $V$  plots, is due to a decrease in  $V_0$  shown in Fig. 2.

These radiation dependent experimental  $C$ - $V$  measurements revealed that in the  $\gamma$ -irradiated diodes, the barrier height  $\Phi_B$  decreases slightly with increase in radiation dose [9,11]. In  $C$ - $V$  measurements only the edge of depletion layer is modulated, and short-wavelength potential fluctuations at the metal–semiconductor interface are screened at the edge of the space-charge region [20,28]. The capacitance ( $C$ ) is insensitive to potential fluctuations at a length scale of less than the space-charge width. In addition, the  $C$ - $V$  technique measures the barrier height of Schottky diode taking averages over the whole area.

There are several methods for the calculation of the density of interface states ( $N_{ss}$ ) [19]. In this study we have used the Hill–Coleman method [29] to obtained the  $N_{ss}$  between metal and semiconductor (Si/SiO<sub>2</sub>) interface. According to this method, the density of interface states can be calculated by using the following equation:

$$N_{ss} = \frac{2}{qA} \frac{(G_m/\omega)_{\max}}{((G_m/\omega)_{\max} C_{ox})^2 + (1 - C_m/C_{ox})^2}, \quad (3)$$

where  $A$  is the area of rectifier contact,  $\omega$  is the angular frequency,  $(G_m/\omega)_{\max}$  is the maximum measured conductance value.  $C_{ox}$  is the capacitance of insulator layer in strong accumulation region. The values of  $C_m$ ,  $R_s$  and  $N_{ss}$  which corresponding to the conductance peak value for MIS Schottky diode determined from  $C$ - $V$  and  $G/\omega$ - $V$  characteristics in the radiation dose range of 0–450 kGy and are given in Table 2. As shown in Table 2, the  $N_{ss}$  increases slightly while the  $R_s$  decreases rapidly with increase in radiation dose.

The conductance technique [19,20,30–32] is based on the conductance losses resulting from the exchange of majority carriers between the interface states and majority carrier band of the semiconductor when a small ac signal is applied to the metal–insulator–semiconductor (MIS) Schottky diodes [16]. The applied ac signal causes the Fermi level to oscillate about the mean positions governed by the dc bias, when the MIS Schottky diode is in the depletion. In Nicollian and Goetzberger's statically theory [16,32], the random distribution of discrete insulator charges and charged interface states in the semiconductor/insulator (Si/SiO<sub>2</sub>) interface plane cause a non-uniform distribution of surface band bending over the interfacial

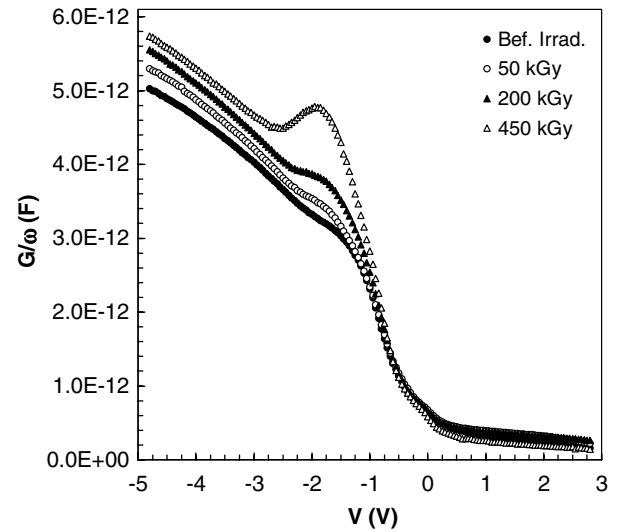


Fig. 4. The  $G/\omega$ - $V$  characteristics of the Al/SiO<sub>2</sub>/p-Si (MIS) Schottky diodes before and after  $\gamma$ -ray irradiation obtained at 1 MHz and room temperature.

plane. Fig. 4 shows the measured  $G/\omega$ - $V$  characteristics of the MIS Schottky diode at various radiation doses between 0 and 450 kGy. The shift of the  $G/\omega$ - $V$  data from inversion toward the accumulation region increases with the increase in radiation dose. Both  $C$ - $V$  and  $G/\omega$ - $V$  characteristics for high frequency (for 1 MHz) applied voltage (Figs. 1 and 4, respectively) were found to have changed with radiation dose.

There are several methods to extract the series resistance of MIS Schottky diode in the literature [33,34]. In this study we have used the conductance method developed by Nicollian and Goetzberger [16,32]. The real series resistance of MIS Schottky diodes can be subtracted from the measured capacitance ( $C_m$ ) and conductance ( $G_m$ ) in strong accumulation region at high frequency ( $f \geq 500$  kHz) [16,32,35,36]. In addition, the voltage and frequency dependence of the series resistance profile can be obtained from the  $C$ - $V$  and  $G/\omega$ - $V$  curves. To determine series resistance  $R_s$ , the MIS Schottky diode is biased into strong accumulation at sufficiently high frequency. The measured impedance ( $Z_m$ ) at strong accumulation of MIS or MOS structure using the parallel RC circuit [20,30] is equivalent to the total circuit impedance as

$$Z_m = \frac{1}{G_m + j\omega C_m}. \quad (4)$$

Table 2

The values of  $C_m$ ,  $R_s$  and  $N_{ss}$  which corresponding to the conductance peak value for MIS Schottky diode determined from  $C$ - $V$  and  $G/\omega$ - $V$  characteristics in the radiation dose range of 0–450 kGy

Irradiation (kGy)	$V_{\max}$ (V)	$C_m$ (F)	$(G_m/\omega)_{\max}$ (F)	$R_s$ ( $\Omega$ )	$N_{ss}$ (eV <sup>-1</sup> cm <sup>-2</sup> )
Before irradiation	-1.95	$9.95 \times 10^{-12}$	$3.29 \times 10^{-12}$	4776.61	$8.14 \times 10^9$
50	-1.90	$1.11 \times 10^{-11}$	$3.48 \times 10^{-12}$	4067.91	$8.61 \times 10^9$
200	-1.85	$1.26 \times 10^{-11}$	$3.82 \times 10^{-12}$	3534.02	$9.45 \times 10^9$
450	-1.80	$1.42 \times 10^{-11}$	$4.73 \times 10^{-12}$	3344.16	$1.17 \times 10^{10}$

Comparing the real and imaginary part of the impedance, the series resistance is given by [20,32,33]

$$R_s = \frac{G_m}{G_m^2 + (\omega C_m)^2}, \quad (5)$$

where  $C_m$  and  $G_m$  represent the measured capacitance and conductance in strong accumulation region.

The series resistance is an important parameter to designate the noise ratio of device as dependent on radiation dose. Therefore, both the real values and voltage dependence of the series resistance  $R_s$  were calculated from Eq. (5) according to [16] and are given in Fig. 5.

As can be seen in Fig. 5, in inversion and depletion regions, the value of the series resistance decreases while in accumulation region almost constant with increasing radiation dose. We considered that the trap charges have enough energy to escape from the traps located between metal and semiconductor interface in the Si band gap.

In addition, the depletion layer width being deduced from the experimental  $C$ – $V$  measurements at high frequency is given by [19,20]

$$W_D = \sqrt{\frac{2\epsilon_s}{qN_A} \Psi_s}, \quad (6)$$

where  $\Psi_s$  is the surface potential and  $N_A$  is the carrier concentration. The  $W_D$  at reverse bias voltage decreases with increasing radiation dose [37].

Fig. 6 shows plots of carrier concentration ( $N_A$ ) and the surface potential ( $\Psi_s$ ) versus radiation dose obtained from the slope of the linear plot of  $C^{-2}$ – $V$  curves. The surface potential ( $\Psi_s$ ) decreases with increasing radiation dose. As can be seen from Figs. 2 and 6, the slope of  $C^{-2}$ – $V$  and, in turn,  $N_A$  increases with increasing radiation dose. This behavior can be explained by whether the interface state charges contribute to the diode capacitance or the charge at the interface states can follow an ac signal. Us-

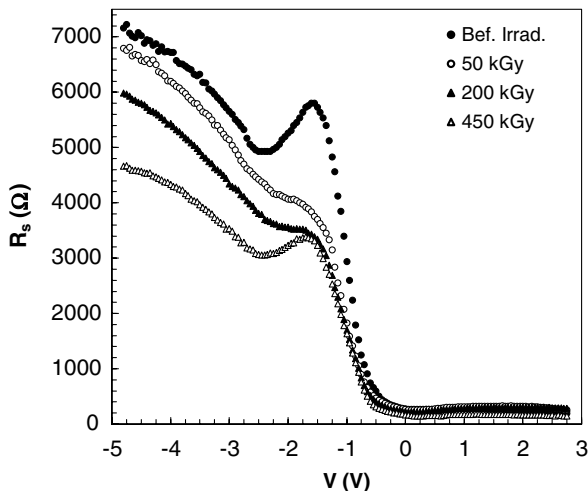


Fig. 5. Series resistance ( $R_s$ ) versus gate bias under different irradiation doses at 1 MHz.

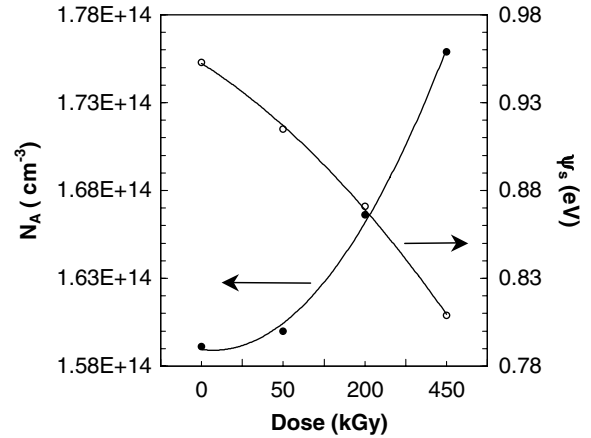


Fig. 6. Carrier concentration ( $N_A$ ) and surface potential ( $\Psi_s$ ) plots obtained from the reverse-bias  $C^{-2}$ – $V$  curves as a function of cumulative  $\gamma$ -ray doses.

ally, at the semiconductor interface, there are various kinds of states with different lifetimes. At low frequencies, all the interface states affected by the applied signal are able to give up and accept charges in response to this signal. The interface state capacitance appears directly in parallel with the depletion capacitance, and this results in a higher total value of the capacitance for Schottky diodes than if no interface states were present [35,38–41].

#### 4. Conclusion

The effect of  $\gamma$ -ray irradiation on the electrical characteristics of p-type MIS Schottky diode has been studied using  $C$ – $V$  and  $G/\omega$ – $V$  measurements. Experimental results show an increase in the change in capacitance and conductance due to the irradiation-induced defects at the interface. Exposure to increasing cumulative  $\gamma$ -ray doses was found to have the following effects: (i) a manifested decreases in the barrier height obtained from  $C$ – $V$  measurements, (ii) decreases in the series resistance  $R_s$  obtained from  $C$ – $V$  and  $G/\omega$ – $V$  measurements and (iii) increase in the interface states  $N_{ss}$  with increasing radiation dose. Such a behavior of  $N_{ss}$  is attributed to the existence of an interfacial insulator layer between the metal and semiconductor that passivates the surface of semiconductor. In summary, it is confirmed that the results of electrical characteristics obtained from  $C$ – $V$  and  $G/\omega$ – $V$  measurements of MIS Schottky diode before radiation is related to the measured values after radiation.

#### References

- [1] T.P. Ma, P.V. Dressendorfer, *Ionizing Radiation Effect in MOS Devices and Circuits*, Wiley, New York, 1989.
- [2] S. Kaschieva, Zh. Todorova, S.N. Dmitriev, *Vacuum* 76 (2004) 307.
- [3] E.A. De Vascancelas, E.F. Da Silva Jr., H. Khoury, V.N. Freire, *Semicond. Sci. Technol.* 15 (2000) 794.
- [4] K.H. Zainninger, A.G. Holmes-Siedle, *RCA Rev.* (1967) 208.
- [5] R. Singh, S.K. Arora, D. Kanjilal, *Mater. Sci. Semicond. Process.* 4 (2001) 425.



- [6] A. Candelori, A. Paccagnella, M. Cammarata, G. Ghidini, M. Ceschia, J. Non-Cryst. Solids 245 (1999) 238.
- [7] M.R. Chin, T.P. Ma, Appl. Phys. Lett. 42 (10) (1983) 883.
- [8] K. Naruke, M. Yoshida, K. Maegushi, H. Tango, IEEE Trans. Nucl. Sci. NS-30 (6) (1983) 4054.
- [9] G.A. Umana-Membreno, J.M. Dell, G. Parish, B.D. Nener, L. Faraone, U.K. Mishra, IEEE Trans. Electron Dev. 50 (12) (2003) 2326.
- [10] T.P. Ma, Semicond. Sci. Technol. 4 (1989) 1061.
- [11] M.Y. Feteiha, M. Soliman, N.G. Gomaa, M. Ashry, Renew. Energy 26 (2002) 113.
- [12] P.S. Winokur, J.M. McGarrity, H.E. Boesch, IEEE Trans. Nucl. Sci. 23 (1976) 1580.
- [13] P.S. Winokur, J.R. Schwank, P.J. McWhorter, P.V. Dressendorfer, D.C. Turpin, IEEE Trans. Nucl. Sci. 31 (6) (1984) 1453.
- [14] J.R. Schwank, P.S. Winokur, F.M. Sexton, D.M. Fleetwood, J.H. Perry, P.V. Dressendorfer, D.T. Sanders, D.C. Turpin, IEEE Trans. Nucl. Sci. 33 (6) (1986) 1178.
- [15] A. Tataroğlu, S. Altındal, S. Karadeniz, N. Tuğluoğlu, Microelectron. J. 34 (2003) 1043.
- [16] E.H. Nicollian, A. Goetzberger, Appl. Phys. Lett. 7 (1965) 216.
- [17] J.C. Bourgoin, J.W. Corbett, Phys. Rev. A 38 (1972) 135.
- [18] L.C. Kimmerling, IEEE Trans. Nucl. Sci. NS-23 (1976) 1497.
- [19] S.M. Sze, Physics of Semiconductor Devices, second ed., John Wiley & Sons, New York, 1981.
- [20] E.H. Nicollian, J.R. Brews, MOS Physics and Technology, John Wiley & Sons, New York, 1982.
- [21] C. Sah, Fundamental of Solid-State Electronics, World Scientific, Singapore, 1991.
- [22] E.H. Rhoderick, R.H. Williams, Metal–Semiconductor Contacts, second ed., Clarendon Press, Oxford, 1978.
- [23] M. Walters, A. Reisman, J. Appl. Phys. 67 (6) (1990) 2992.
- [24] T. Chen, Z. Luo, J.D. Cressler, T.F. Isaacs-Smith, J.R. Williams, G. Chung, S.D. Clark, Solid State Electron. 46 (2002) 2231.
- [25] E.A. De Vascancelas, E.F. Da Silva Jr., Semicond. Sci. Technol. 12 (1997) 1032.
- [26] K.K. Hung, Y.C. Cheng, J. Appl. Phys. 62 (1987) 4204.
- [27] B. Akkal, Z. Benamara, B. Gruzza, L. Bideux, Vacuum 57 (2000) 219.
- [28] P. Cova, A. Singh, Solid State Electron. 33 (1) (1990) 11.
- [29] W.A. Hill, C.C. Coleman, Solid State Electron. 23 (9) (1980) 987.
- [30] P. Chattopadhyay, A.N. Daw, Solid State Electron. 29 (1986) 555.
- [31] A. Singh, Solid State Electron. 28 (1985) 223.
- [32] E.H. Nicollian, A. Goetzberger, Bell Syst. Tech. J. 46 (1967) 1055.
- [33] H. Norde, J. Appl. Phys. 50 (1979) 5052.
- [34] K. Sato, Y. Yasamura, J. Appl. Phys. 58 (1985) 3656.
- [35] A. Tataroğlu, Ş. Altındal, Microelectron. Eng. 83 (2006) 582.
- [36] K.K. Hung, Y.C. Cheng, J. Appl. Phys. 62 (1987) 4204.
- [37] J.W. Stacey, R.D. Schrimpf, D.M. Fleetwood, K.C. Holmes, IEEE Trans. Nucl. Sci. 51 (6) (2004) 3686.
- [38] R.K. Chauhan, P. Chakrabarti, Microelectron. J. 33 (2002) 197.
- [39] A. Ziel, Solid State Physical Electronics, second ed., Prentice-Hall, New Jersey, 1968.
- [40] S. Chand, J. Kumar, J. Appl. Phys. A 63 (1996) 171.
- [41] W.M.R. Divigalpitiya, Solar Energy Mater. 18 (1989) 253.